Project no. 316488

Project Acronym: **KESTCELLS**

Project title: Training for suitable low cost PV technologies: development of kesterite based efficient solar cells. Industry-Academia Partnerships and Pathways

Start date of project: 01/09/2012

Duration: 48 months

Project coordinator: Dr. Edgardo Saucedo

Project coordinator organization name: IREC

Project website address: www.kestcells.eu

Deliverable D1.2

Identification of Raman active vibrational modes of CZTS and CZTSe

Delivery date: Month 16 (December 2013)

Dissemination Level	
PU	Public

Document details:	
Workpackage	WP1: Fundamental properties of Kesterites
Partners	IREC
Authors	M. Dimitrievska, V. Izquierdo-Roca, A. Pérez-Rodríguez
Document ID	D1.2
Release Date	24/02/2014

Identification of Raman active vibrational modes of CZTS and CZTSe

1. Introduction

Polycrystalline kesterite $Cu_2ZnSn(S,Se)_4$ (CZTS, CZTSe) thin films have recently drawn much attention as being a promising candidate as an absorber layer in solar cell technologies[1-3], and devices have already reached a conversion efficiency of 12.6%[4] based on the related $Cu_2ZnSn(S,Se)_4$ compound. Optoelectronic properties of solar cells are strongly dependent on the structural properties, crystalline quality, and presence of secondary phases in the absorber layer[5-8].

Raman spectroscopy is one of the most powerful tools for determining the crystalline structure and quality of semiconductor thin films, since the shape and position of Raman peaks are strongly influenced by the presence of defects in the material, either in the form of structural inhomogeneities or secondary phases[9-12]. In order to achieve better device performance in solar cells based on CZTS and CZTSe absorbers and to improve the usage of Raman spectroscopy as a control method for assessment of crystalline quality and identification of secondary phases in these promising emerging compound semiconductors, it is necessary to obtain better knowledge of their vibrational properties. Theoretical calculations on band structure, optical properties, and intrinsic defects have recently been reported[13-16]. First principle calculations done by Khare[17] and Gurel[18] have given theoretical predictions on the positions of all Raman active optical modes of the kesterite structure with the space group $I\bar{4}$ ($\Gamma = 3A \oplus 6B \oplus 6E$).

Usually, experimental studies for determining the Raman peaks of ksterites are done with the use of green excitation (514.5 or 532.0 nm), which is standard in Raman spectroscopy[9, 19, 20]. On the other hand, identification of secondary phases in kesterite compounds in some cases cannot be done with the use of green excitation, but rather requires the use of different excitation wavelengths leading to near resonant excitation conditions for certain secondary phase compounds and they enable enhancement of their modes for more straightforward detection[10]. For example, ultraviolet (UV) excitation allows very sensitive detection of ZnS which is the most expected secondary phase in Zn rich and Cu poor device grade CZTS layers[21], while blue excitation (457.8 nm) allows very easy identification of ZnSe on CZTSe layers[22]. Development of Raman scattering based procedures for detection of secondary phases in kesterite based compounds is of strong interest, because of the high impact of these phases on the optoelectronic properties of the solar cells. Detection of CZT(S,Se) and secondary phases as Zn(S,Se) by standard techniques such as x-ray diffraction is strongly compromised by the high level of overlapping of the main peaks in the diffractograms characteristics for these phases.

While use of different excitation wavelengths allows identification of secondary phases, they can also induce changes in the intensities of the optical Raman modes of CZT(S,Se). For example, some Raman modes which could not be observed with standard excitation could appear with much higher intensity in the spectra measured under nonstandard excitations, and this might lead in some cases to misinterpretation with modes of secondary phases. Thus, it is important first to study the behavior of all Raman modes of CZT(S,Se) in relation to different excitations, before applying this method for identification of secondary phases. Here, we perform a detailed study of the whole spectral range where

first order Raman CZT(S,Se) modes are theoretically expected (from 50 cm^{-1} up to 400 cm^{-1}), and we also extend the range of excitation wavelengths to the UV and near infrared (NIR) regions.

In this framework, this report describes a complete analysis and identification of all active Raman modes for polycrystalline CZT(S,Se) thin films using six different excitation wavelengths (325.0, 457.9, 514.5, 632.8, 785.0, 830.0 nm). In principle, near resonance Raman effects are expected to be the main factors influencing changes in the Raman spectra of CZT(S,Se) with the excitation wavelength. Tuning the incident laser to resonate with a strong electronic inter-band transition enables the enhancement of the Raman cross section, and vibrational modes associated with that particular transition exhibit an increase in intensity[23].

2 Experimental Details

CZT(S,Se) thin films of photovoltaic grade with high crystalline quality were investigated. The samples were prepared by thermal treatment of metallic precursors made by DC-magnetron sputtering deposition onto soda-lime glass/Mo substrates. Prototype solar cell devices made with these films give promising efficiency values up to 7.2%. More details about precursor deposition, thermal processing, device fabrication, and characterization can be found elsewhere[21]. Compositional ratios of the as-annealed films were approximately Cu/(Zn+Sn) = 0.80 and Zn/Sn = 1.20. These non-stoichiometric composition conditions are typically required to achieve devices with reasonable efficiency[8]. These conditions inhibit formation of detrimental Cu-Sn-S ternary phases, although they might favour formation of the Zn(S,Se) secondary phase. To remove these secondary phases from the surface of the films, a selective chemical etching for ZnS and ZnSe has been performed according with the processes explained in [24] and [25], for the CZTS and CZTSe thin films respectivlly. After etching with these solutions, the composition ratios change to values closer to a stoichiometric composition (Cu/(Zn+Sn) = 0.96 and Zn/Sn = 1.09). The spectra presented in this letter correspond to the as-etched samples. As previously reported[21], Zn-excess remaining in the etched film tends to be mainly concentrated at the back contact region, and we can consider that the surface is free of ZnS and ZnSe. This is corroborated by Raman scattering measurements performed with UV and blue excitations, as will be discussed later.

Raman scattering measurements were performed in back scattering configuration with a LabRam HR800-UV and T64000 Horiba-Jobin Yvon spectrometers. For the HR800-UV system, diode lasers with wavelengths of 785.0 and 830.0 nm, and gas HeCd and HeNe lasers with wavelengths of 325.0 and 632.8 nm, respectively, were used for excitation. In this system, excitation and light collection were made through an Olympus metallographic microscope, with a laser spot size on the order of 1- 2μm (depending on the excitation wavelength). To avoid effects in the spectra related to potential microscopic inhomogeneities, the spot was rastered over an area of 30 x 30 μm^2. Furthermore, the T64000 system works coupled with an ion-Ar^+ laser, and measurements were made with 514.5 nm and 457.9 nm excitation lines, with a 100 μm spot size on the sample. In all cases, and to avoid the presence of thermal effects in the spectra, the power excitation density applied was lower than 50 W/cm^2. The first-order Raman spectrum of monocrystalline Si was measured as a reference before and after acquisition of each Raman spectrum, and the spectra were corrected with respect to the Si line at 520 cm^{-1}.

3 Results and discussion.

3.1 Vibrational properties of CZTS thin films

According to theoretical calculations for electronic band structure of kesterites done by Kumar and Persson[26] the estimated energy, for CZTS, of the Γ_1 point (band gap energy) is 1.47 eV, while the energy of the Γ_2 point is around 3.50 eV. Taking into account the values of energies for Γ_1 and Γ_2 points, the excitation wavelengths of 830.0, 785.0, and 325.0 nm, with corresponding energies of 1.49, 1.58, and 3.82 eV could be considered as good conditions for near resonance Raman scattering effects. In principle, increasing in intensity of the Raman modes because of near resonant excitation conditions is expected to take place especially for E and B symmetry modes which are NIR active and have TO/LO splitting due to their polar character[17, 23]. It is interesting to remark that these modes are only observed as very weak peaks in standard Raman scattering conditions, where the spectra are dominated by the two main A symmetry modes at 287 and 338 cm^{-1}, which are not NIR active.

Figure 1 presents the experimental Raman spectra of measured CZTS sample under different excitation wavelengths. Simultaneous fittings of spectra with Lorentzian curves have allowed identification of 18 peaks attributed to the 27 optical modes which are expected according to the zone center phonon representation. The position of each Raman peak, the excitation condition under which it is most intense, and symmetry assignment is presented in Table I. In addition, Table I also contains theoretical calculations[17, 18] and previously reported experimental data[9,19,20]. The symmetry assignment of Raman modes was done by comparing the experimentally obtained frequencies with the reported references as well as with polarization measurements done for these samples. Inset in figure 1 shows the Raman spectra measured with 325 nm excitation wavelength in the CZTS sample and in a reference ZnS sample, in the 500 – 1150 cm^{-1} spectral range. The spectrum from the reference ZnS sample shows the peaks at 697 and 1045 cm^{-1} corresponding to the second and third order peaks of the main ZnS Raman mode. Presence of these peaks is due to the existence of a quasi-resonant excitation of the main ZnS Raman mode at this excitation wavelength[10]. Absence of these peaks characteristic of the ZnS phase from the spectrum measured in the CZTS layer corroborates the absence in the surface region of this layer of a ZnS secondary phase. Additionally, the CZTS second (region between 550-750 cm^{-1}) and third (region between 900-1050 cm^{-1}) spectral regions are also observed in the spectrum, including the second and third order CZTS peaks at 670.9 and 1004.7 cm^{-1}, respectively.

Figure 2 shows a plot of the spectra measured with 325.0, 514.5 nm, 632.8 and 785.0 nm excitation wavelengths normalized to the intensity of the main peak at 337.5 cm^{-1}. Spectra measured with 325.0 nm are characterized by a strong increase in the relative intensity of the Raman peaks at 255.1, 271.1, 315.9 and 347.3 cm^{-1} in relation to those from the spectra measured with standard 514.5 nm excitation. Similarly, relative intensity of peaks at 139.8, 150.7, 262.7, 366.6 and 374.4 cm^{-1} increase for 785.0 nm excitation. These results agree with the expected enhancement in the intensity of CZTS polar vibrational modes taking into account the possible existence of a near resonant behavior. In addition, spectra measured with 632.8 nm also show an increase in the relative intensity of the peaks that are located at 81.5, 96.9, 262.7, and 366.6 cm^{-1}. This could be due to the existence also of the near resonant excitation behavior, even if the energy is not so close to those of the Γ_1 and Γ_2 CZTS points.

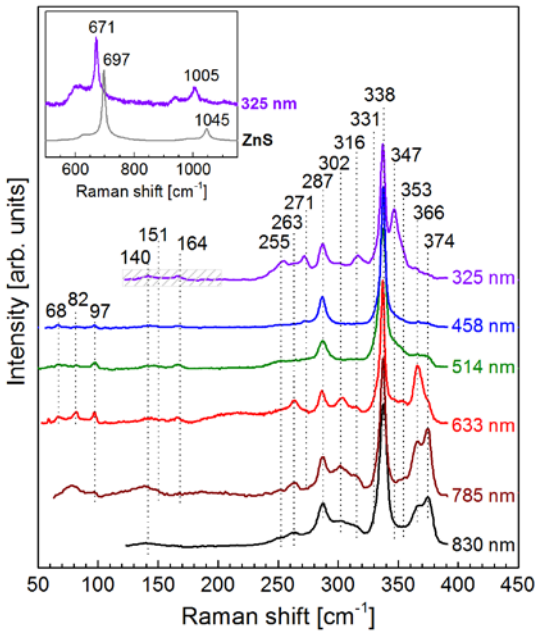

Figure 1: Raman spectra of polycrystalline Cu_2ZnSnS_4 (CZTS) thin film measured with different excitation wavelengths with indication of the characteristic peaks. Dashed region presented in the spectrum measured with 325 nm wavelength corresponds to the region of strong attenuation originating from the Raman edge filter. Presence of Raman peaks in this region suggests strong enhancement of the modes expected in this spectral interval. Spectra are arbitrarily vertically shifted for more clarity. Inset shows the spectra measured in the 500-1150 cm^{-1} region with 325 nm excitation wavelength from the CZTS thin film and a reference ZnS layer.

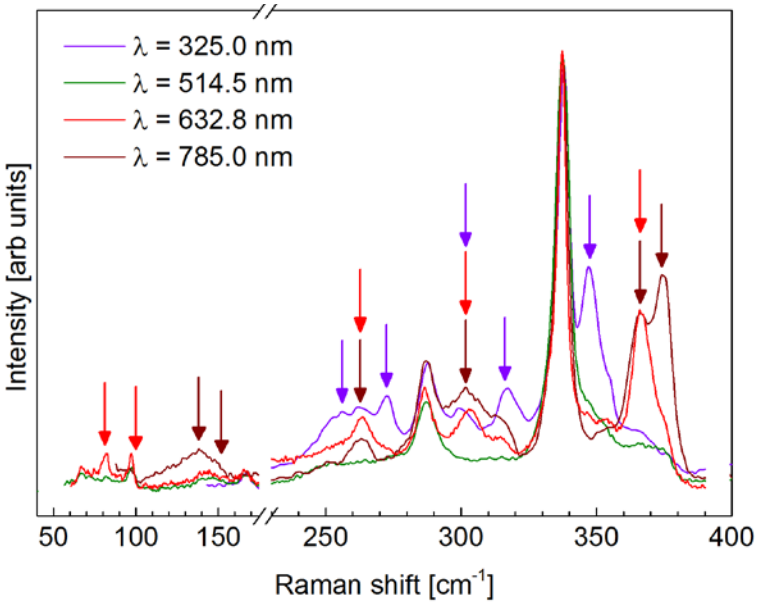

Figure 2: Comparison between Raman spectra measured with standard green excitation (514.5 nm), and measurements made with 325.0, 632.8 and 785.0 nm excitation. The colored arrows indicate the excitation wavelength for which each particular band has the greatest increase in intensity.

Table I. Frequency (in cm^{-1}) of peaks from simultaneous fitting of Raman spectra of CZTS thin films measured with different excitation wavelengths, excitation condition under which the peak is best resolved, and proposed mode symmetry assignment. These are compared with theoretical predictions [17,18] and other reported experimental data [9,19,20].

This work			Theoretical predictions		Experimental reported		
λ^a [nm]	RS^b [cm^{-1}]	Sym^c	RS^d [cm^{-1}]	RS^e [cm^{-1}]	RS^f [cm^{-1}]	RS^g [cm^{-1}]	IR^h[cm^{-1}]
633	67.8	E	79.2 E(TO/LO)	82.2 E(TO/LO)	66		68 (IR)
633	81.5	B	92.3 B(TO)/ 93.1 B(LO)	87.8 B(TO)/ 88.2 B(LO)	83		86 (IR)
633	96.9	E/B	101.4 E(TO/LO)/ 104.2 B(TO)/ 104.3 B(LO)	99.3 B(TO/LO)/ 102.9 E(TO)/ 103.0 E(LO)	97		
785	139.8	E	166.1 E(TO)	150.0 E(TO)	143	143 E(TO)	143 (IR)
785	150.7	E	166.2 E(LO)	150.5 E(LO)		145 E(LO)	
325	164.1	B	179.6 B(TO)/ 179.9 B(LO)	168.2 B(TO)/ 169.5 B(LO)	166	160 B(TO) 162 B(LO)	168 (IR)
325	255.1	B/E	269.1 B(TO)/ 278.2 E(TO)	237.9 B(TO)/ 247.8 E(TO)	252	245 B(TO) 250 B(LO) 255 E(LO)	255 (IR)
633	262.7	B	285.1 B(LO)	253.7 B(LO)			
325	271.1	E	289.8 E(LO)	254.8 E(LO)	272		293(IR)
830	287.1	A	302.1 A	281.7 A	287	285 A	
785	302.1	A	309.0 A	270.0 A		306 A	
325	315.9	E	309.7 E(TO)/ 314.1 E(LO)	278.0 E(TO)/ 290.5 E(LO)			316 (IR)
325	331.9	B	332.7 B(TO)/ 336.1 B(LO)	307.6 B(TO)/ 311.4 B(LO)			
514	337.5	A	335.2 A	338.5 A	337	334 A	
325	347.3	E	341.4 E(TO)	351.1 E(TO)	347	341 E(TO) 346 E(LO)	
514	353.0	B	354.8 B(TO)	357.0 B(TO)	353	352 B(TO) 353 B(LO)	351 (IR)
633	366.6	E	353.3 E(LO)	365.3 E(LO)			
785	374.4	B	366.4 B(LO)	373.6 B(LO)			

λ^a is the excitation wavelength

RS^b is the Raman shift from this work

Sym^c is the symmetry proposed in this work

$RS^{d,e,f,g}$ are the Raman shift reported in references [17], [18], [9], [19],

IR^h are the Infrared absorption frequencies reported in [20]

In addition, these excitation conditions also allow observation of a well resolved peak at 302.1 cm^{-1}, that according to simulation data, has been identified as the third A symmetry mode from the CZTS kesterite phase[19]. Even though Dumcenco[19] already reported the existence of this mode, it is interesting to remark that in their work the presence of this mode was deduced from deconvolution of the experimental spectra, and the peak was not experimentally resolved in their spectra, as is done here.

In the case of the peak at 347.3 cm^{-1} observed with UV excitation conditions, an increase in the intensity of a peak in this spectral region has previously been attributed to the presence of a ZnS secondary phase, because of the existence of a quasi-resonant excitation of ZnS in these measuring conditions[10]. However, experimentally, presence of this phase is also accompanied by the detection of the second order ZnS peak at 697 cm^{-1} spectral region. Absence of this second order peak in the spectra form the samples analyzed in this work (as shown in the inset in Figure 1) supports its identification as a mode characteristic of the CZTS compound, unrelated to the presence of a ZnS secondary phase.

On the other hand, fitting of the spectra gives also a contribution at 331.9 cm^{-1} , which has been identified with a B symmetry mode, in agreement with the theoretical data. However this is also close to a peak at 331 cm^{-1} which has been related to the presence of local inhomogeneities with a high degree of disorder in the cation sublattice of CZTS, as reported by Fontané et al[9] for bulk powder samples. More recent studies from single crystal bulk samples with different compositions[27] have identified this peak with the main A_1 symmetry mode from the disordered kesterite phase, which is characterized by a random distribution of Cu and Zn cations in the Cu-Zn planes. This leads to a change in the group symmetry to the stannite-like $I\bar{4}m2$. In contrast with the behavior shown in Figure 2, presence of this disordered kesterite phase in the bulk and single crystal samples reported in refs. [9,27] is characterized by an intense and broad peak in this spectral region in the spectrum measured with 514.5 nm excitation. This suggests that conditions related to the growth of bulk samples, which typically involve higher temperature thermal treatments than those used for the synthesis of the device grade polycrystalline thin films, favor formation of this disordered phase when working under non-stoichiometric conditions.

Confirmation of proposed symmetry types could be done with comparison to polarized Raman spectra measurements for CZTS, as seen in Figure 3. According to Raman tensors for the space group $I\bar{4}$ [17] and calculations of depolarization ratio for the polycrystalline films with random orientation, in the case of change in polarization conditions from parallel $\langle Z|XX|Z\rangle$ to perpendicular $\langle Z|XY|Z\rangle$ configurations, the intensity of all A modes would always decrease, while the intensity of all E modes would always increase. In case of B modes their intensity could increase or decrease depending on their type. From the results shown in Figure 3, it can be seen that intensities of all peaks increase with the change in polarization, expect for peaks in spectral region from 270 to 340 cm^{-1} which decrease in intensity. This indicates that all A modes must be positioned in this region, which is in accord with the multiwavelength excitation results.

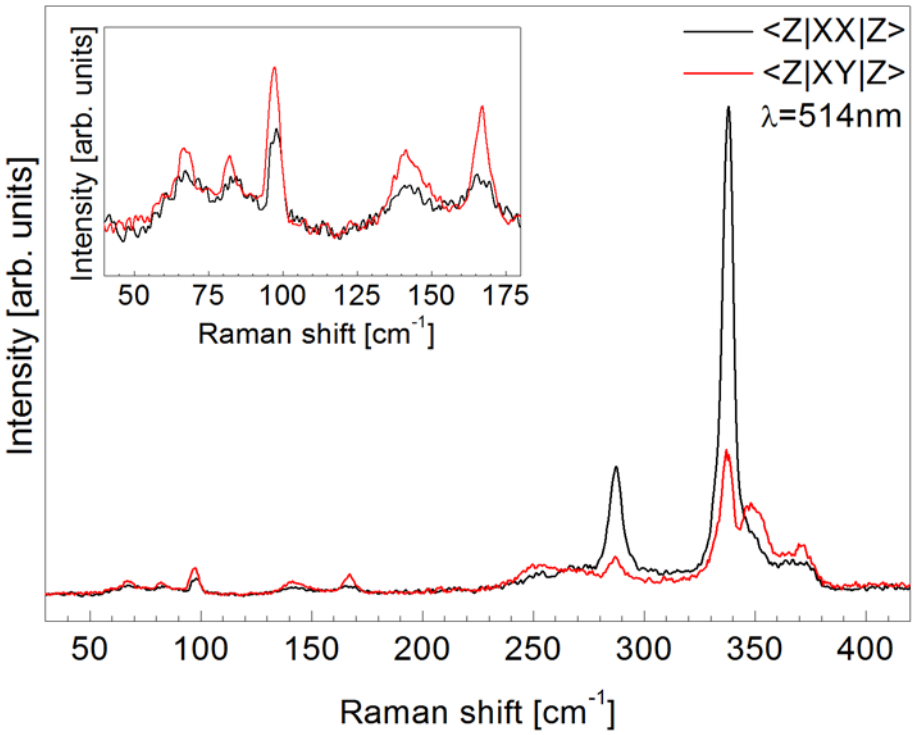

Figure 3: Raman polarization measurements of CZTS done in parallel and perpendicular polarization configurations (excitation wavelength 514.5 nm)

3.2 Vibrational properties of CZTSe

According to theoretical calculations for electronic band structure of CZTSe done by Kumar and Persson in [24] the estimated energy of Γ_1 point (band gap energy) is 0.9 eV, while the energy of Γ_2 point is 3.0 eV. Taking into account the values of energies for Γ_1 and Γ_2 points, and in contrast to CZTS, the used excitation wavelengths are not considered as good conditions for near resonance Raman scattering effects in case of CZTSe, expect in the case of NIR expiations, where an incraise in intensity of polar modes is expected.

Similarly to the case of CZTS, Figure 4 presents the experimental Raman spectra of measured CZTSe sample under different excitation wavelengths. Simultaneous fittings of spectra with Lorentzian curves have allowed identification of 17 peaks attributed to the 27 optical modes which are expected according to the zone center phonon representation. The position of each Raman peak, the excitation condition under which it is most intense, and symmetry assignment is presented in Table II. In addition, Table II also contains theoretical calculations[17, 18] and previously reported experimental data[28, 29]. The symmetry assignment of Raman modes was done by comparing the experimentally obtained frequencies with the reported references as well as applaying the same rules for the mode behaviour as in the case of CZTS to the polarization measurements done for these samples (figure 6).

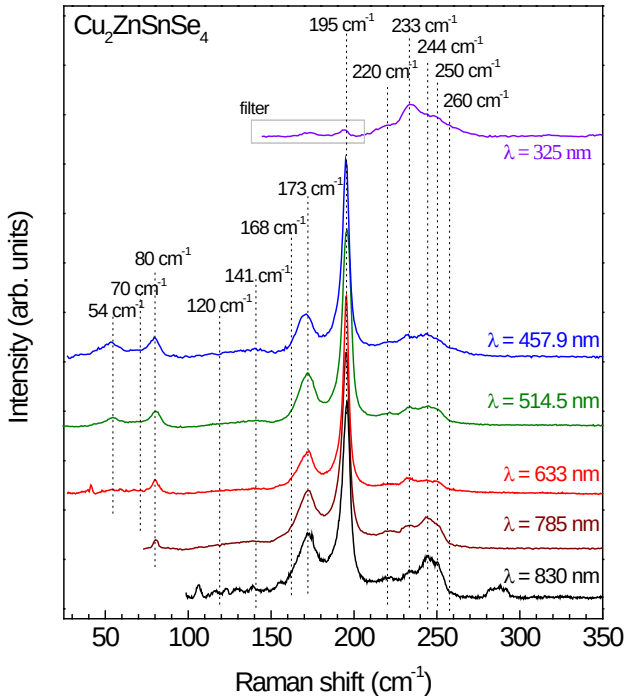

Figure 5: Raman spectra of polycrystalline $Cu_2ZnSnSe_4$ (CZTSe) thin film measured with different excitation wavelengths with indication of the characteristic peaks. Dashed region presented in the spectrum measured with 325 nm wavelength corresponds to the region of strong attenuation originating from the Raman edge filter. Presence of Raman peaks in this region suggests strong enhancement of the modes expected in this spectral interval. Spectra are arbitrarily vertically shifted for more clarity.

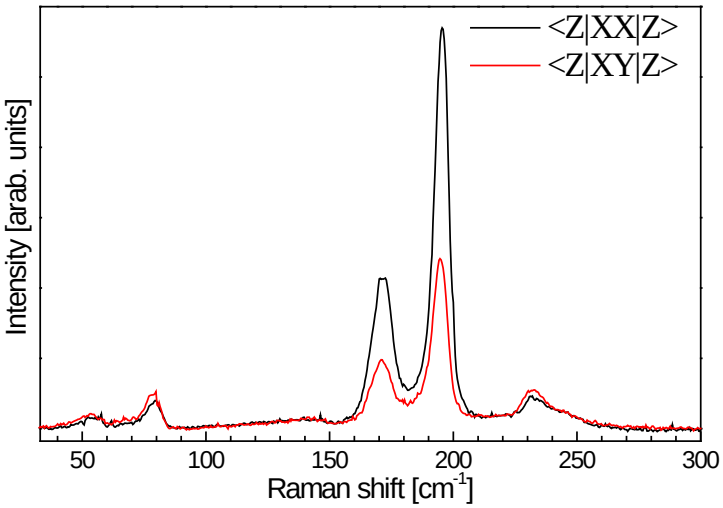

Figure 6: Raman polarization measurements of CZTSe done in parallel and perpendicular polarization configurations (excitation wavelength 514.5 nm)

Table II. Frequency (in cm^{-1}) of peaks from simultaneous fitting of Raman spectra of CZTSe thin films measured with different excitation wavelengths, excitation condition under which the peak is best resolved, and proposed mode symmetry assignment. These are compared with theoretical predictions [17,18] and other reported experimental data [refernce].

This work			Theoretical predictions		Experimental reported	
λ^a [nm]	RS^b [cm^{-1}]	Sym^c	RS^d [cm^{-1}]	RS^e [cm^{-1}]	RS^f [cm^{-1}]	RS^g [cm^{-1}]
514	54.4	E	60.6 E(TO/LO)	62.6 E(TO)/ 62.7 E(LO)		51
514	69.6	B	74.4 B(TO)/ 74.6 B(LO)	73.6 B(TO)/ 73.8 B(LO)		
785	79.2	B	85.4 B(TO)/ 85.6 B(LO)	83.0 B(TO)/ 83.5 B(LO)	77 B(TO/LO)	77
785	81.7	E	81.0 E(TO/LO)/	82.8 E(TO)/ 82.9 E(LO)	82 E(TO/LO)	
514	138.5	E	159.0 E(TO)/ 159.1 E(LO)	141.1 E(TO)/ 141.8 E(LO)	138 E(TO/LO)	
785	156.9	B	171.5 B(TO)/ 171.8 B(LO)	156.7 B(TO)/ 157.3 B(LO)	157 B(TO/LO)	
785	171.9	A	181.0 A	162.8 A	170 A	168
785	174.5	A	183.6 A	166.5 A	174 A	171
785	177.4	B	202.5 B(TO) / 211.3 B(LO)	175.3 B(TO)/ 178.7 B(LO)	178 B(TO/LO)	
785	192.0	E	205.4 E(TO)/ 208.8 E(LO)	179.0 E(TO)/ 180.5 E(LO)	189 E(TO/LO)	
785	196.8	A	196.2 A	186.3 A	196 A	195
325	220.6	E	217.4 E(TO)	199.8 E(TO)	224 E(TO)	
785	231.9	E	219.9 E(LO)	202.8 E(LO)	231 E(LO)	231
325	234.2	B	223.4 B(TO)	204.2 B(TO)	235 B(TO)	
785	239.7	B	226.0 B(LO)	205.4 B(LO)	239 B(LO)	
325	248.3	B	231.0 B(TO)	227.1 B(TO)	245 B(TO)	244
325	250.8	B	236.0 B(LO)	228.8 B(LO)	250 B(LO)	

λ^a is the excitation wavelength

RS^b is the Raman shift from this work

Sym^c is the symmetry proposed in this work

$RS^{d,e,f,g}$ are the Raman shift reported in references [17], [18], [28], [29]

4. Conclusions

In conclusion, this work demonstrates the utility of multiwavelength excitation for the deeper vibrational characterization of device grade polycrystalline CZT(S,Se). In addition to allowing easier identification of peaks previously observed with standard green excitation, the analysis performed here also allows experimental observation and symmetry assignment of new Raman peaks characteristic for CZT(S,Se) compounds, which were not previously experimentally reported, but are theoretically predicted. In the end this methodology has allowed indetification of 18 peaks for CZTS and 17 peaks for CZTSe which are attributed to 27 optical modes theriticlly predicted for these kind of compounds. The developed methodology of using different excitation lengths is especially usuful, since it is enchancing the weak peaks which are difficult to observe in standartd conditions. This knowledge is especially relevant for the further development of multiwavelength Raman scattering based methodologies for detection of secondary phases, which is still required for further optimization of these technologies.

References

[1]C. A. Wolden, J. Kurtin, J. B. Baxter, I. Repins, S. E. Shaheen, J. T. Torvik, A. A. Rockett, V. M. Fthenakis, and E. S. Aydil, J. Vac. Sci. Technol. A 29, 030801 (2011).

[2]H. Katagiri, Thin Solid Films 480–481, 426 (2005).

[3]T. Kato, H. Hiroi, N. Sakai, S. Muraoka, H. Sugimoto, 27th European PV Solar Energy Conf. and Exhibition, 2236 (2013).

[4]W. Wang, M. T. Winkler, O. Gunawan, T. Gokmen, T. K. Todorov, Y. Zhu, and D. B. Mitzi, "Device Characteristics of CZTSSe Thin-Film Solar Cells with 12.6% Efficiency," Adv. Energy Mater., p. n/a–n/a (2013).

[5]S. Schorr, Sol. Energy Mater. Sol. Cells 95, 1482–1488 (2011).

[6]A. Redinger, D.M. Berg, P.J. Dale, and S. Siebentritt, J. Am. Chem. Soc. 133, 3320 (2011).

[7]S. Chen, X.G. Gong, A. Walsh, and S.-H. Wei, Appl. Phys. Lett. 96, 021902 (2010).

[8]D. B. Mitzi, O. Gunawan, T. K. Todorov, K. Wang, S. Guha, Sol. Energy Mater. Sol. Cells 95, 1421 (2011).

[9]X. Fontane, V. Izquerdo-Roca, E. Saucedo, S. Schorr, V.O. Yukhymchuk, M. Ya. Valakh, A. Perez-Rodrigez, J.R. Morante, J. Alloys Compd. 539, 190 (2012).

[10]X. Fontané, L. Calvo-Barrio, V. Izquierdo-Roca, E. Saucedo, A. Pérez-Rodriguez, J.R. Morante, D.M. Berg, P.J. Dale, and S. Siebentritt, Appl. Phys. Lett. 98, 181905 (2011).

[11]A.-J. Cheng, M. Manno, A. Khare, and C. Leighton, S. A. Campbell, and E.S. Aydil, J. Vac. Sci. Technol. A 29, 051203 (2011).

[12]P.A. Fernandes, P.M.P. Salome, A. F. da Cunha, J. Alloys Compd. 509, 7600-7606 (2011).

[13]S. Chen, X. G. Gong, A. Wals and S. H. Wei, Phys. Rev. B 79, 165211 (2009).

[14]C. Persson, J. Appl. Phys. 107, 053710 (2010).

[15] A. Nagoya, R. Asahi, R. Wahl and G. Kresse, Phys. Rev. B 81, 113202 (2010).

[16] S. Chen, J. H. Yang, X. G. Gong, A. Walsh and S. H. Wei, Phys. Rev. B 81, 245204 (2010).

[17]T. Gurel, C. Sevik, T. Cagin, Phys. Rew. B, 84, 205201 (2011).

[18]A. Khare, B. Himmetoglu, M. Cococcioni, E.S. Aydil, J. Appl. Phys. 111, 123704 (2012).

[19]D. Dumcenco and Y.-S. Huang, Opt. Materials 35, 419-425 (2013).

[20]M. Himmrich and H. Haeuseler, Spectro. Chimica Acta 47A, 933 (1991).

[21]A. Fairbrother, X. Fontané, V. Izquierdo-Roca, M. Espíndola-Rodríguez, S. López, M. Placidi, L. Calvo-Barrio, A. Pérez-Rodríguez and E. Saucedo, Sol. Energy Mater. Sol. Cells 112, 97-105 (2013).

[22] Chem. Eur. J. 19, 14814 – 14822 (2013).

[23]P. Y. Yu, M. Cardona, "Fundamentals of Semiconductors", 4th edition, Springer, Berlin, 401 (2010).

[24]A. Fairbrother, E. Gracia-Hemme, V. Izquierdo-Roca, X. Fontane, F. A. Pulgarin-Agudelo, O. Vigil-Gala, A. Perez-Rodrigez and E. Saucedo, J. Am. Chem. Soc. 134, 8018 (2012).

[25] A. Redinger, K. Hönes, X. Fontané, V. Izquierdo-Roca, E. Saucedo, N. Valle, A. Pérez-Rodríguez, and S. Siebentritt, Appl. Phys. Lett., 98, 10, 101907 (2011).

[26]M. Kumar and C. Persson, International Journal of Theoretical and Applied Sciences, 5(1), 1 (2013).

[27]M.Y. Valakh, O. F. Kolomys, S. S. Ponoaryov, V. O. Yukhymcuk, I. S. Babichuk, V. Izquierdo-Roca, E. Saucedo, A. Perez Rodrigez, J. R. Morante, S. Schorr and I. V. Bodnar, Phys. Status Solidi RRL 1 (2013).

[28]M. Guc, S. Levcenko, V. Izquerdo-Roca, X. Fontane, E. Arshanov, A. Perez-Rodrigez, J. Appl. Phys. 114, 173507 (2013).

[29]R. Djemour, A. Rediger, M. Mousel, L. Gutay, X. Fontane, V. Izquerdo-Roca, A. Perez-Rodrigez, S. Siebentritt, Optics Exprss 21, S4 (2013).

D1.2 Deliverable: Summary

This work presents a complete analysis of all Raman active modes of $Cu_2ZnSn(S,Se)_4$ measuring with six different excitation wavelengths from NIR to UV. Simultaneous fitting of spectra allowed identification of 18 peaks for CZTS and 17 peaks for CZTSe from device grade layers with composition close to stoichiometry that are attributed to the 27 optical modes theoretically expected for this crystalline structure, including detection of new peaks not observed previously, but theoretically predicted. Resonance effects are assumed to explain the observed increase in intensity of weak modes for UV and NIR excitations. This knowledge is especially relevant for the further development of multiwavelength Raman scattering based methodologies for detection of secondary phases, which is still required for further optimization of these technologies.

This work demonstrates the utility of multiwavelength excitation for the deeper vibrational characterization of device grade polycrystalline CZT(S,Se). The results presented in this deliverable have been published in the paper “Multiwavelength excitation Raman scattering study of polycrystalline kesterite Cu2ZnSnS4 thin films” by M. Dimitrievska et al. (Appl. Phys. Lett. 104, 021901 (2014)) and in the frame of KESTCELLs project.